

Laser-Induced Fluorescence Excitation Spectra of *tert*-Butoxy and 2-Butoxy Radicals

Chuji Wang, Liat G. Shemesh, Wei Deng, Michael D. Lilien, and Theodore S. Dibble\*

Department of Chemistry, College of Environmental Science and Forestry, State University of New York, 1 Forestry Drive, Syracuse, New York 13210

Received: June 3, 1999; In Final Form: August 16, 1999

Laser-induced fluorescence (LIF) excitation spectra of *t*-C<sub>4</sub>H<sub>9</sub>O (*tert*-butoxy) and 2-C<sub>4</sub>H<sub>9</sub>O (2-butoxy) radicals were investigated in the wavelength range 335–400 nm. The radicals were formed by laser photolysis of the corresponding butyl nitrites at 355 nm. For *tert*-butoxy, 16 vibronic bands in two progressions were labeled. The dominant progression corresponds to C–O stretching mode with  $\nu'_{\text{C-O}} = 521 \pm 10 \text{ cm}^{-1}$ . The transition origin was tentatively assigned at  $25\,866 \text{ cm}^{-1}$  (386.6 nm). Numerous bands remain unassigned. The LIF excitation spectrum of 2-butoxy, consisting of 15 vibronic bands in four progressions, was observed for the first time. A C–O stretching frequency  $\nu'_{\text{C-O}} = 567 \pm 10 \text{ cm}^{-1}$  was obtained from the dominant progression. The transition origin was tentatively assigned at  $26\,185 \text{ cm}^{-1}$  (381.9 nm). Three other progressions are evident, which have different vibrational band intervals:  $617 \pm 10$ ,  $590 \pm 10$ , and  $552 \pm 10 \text{ cm}^{-1}$ . Zero-pressure fluorescence lifetimes for numerous vibronic bands of *tert*-butoxy and 2-butoxy were determined to be about 150 and 85 ns, respectively. These spectra can be used as a convenient spectroscopic tool for kinetic studies of butoxy radicals and should provide a starting point for investigations of their excited states structure and dynamics.

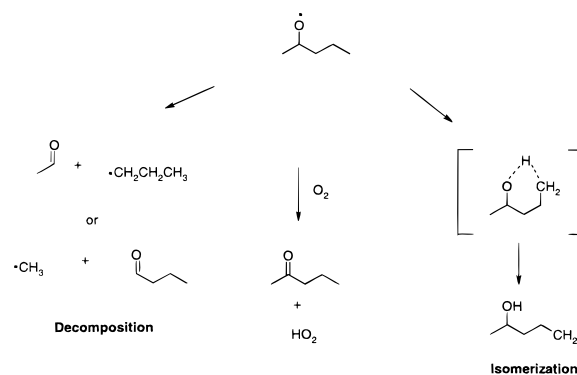
## I. Introduction

Alkoxy radicals are central intermediates in the atmospheric degradation of volatile organic compounds as well as fascinating targets of basic research. The fate of alkoxy radicals in the atmosphere influences the yield of ozone, air toxics, and organic aerosol in polluted air.<sup>1</sup> Alkoxy radical chemistry in the atmosphere is dominated by three reactions, as illustrated in Scheme 1.<sup>2,3</sup> The existence of multiple reaction pathways for alkoxy radicals complicates efforts to understand the atmospheric degradation pathways of volatile organic compounds and their effects on air quality.

The present understanding of alkoxy radical kinetics is built primarily on product yield studies, and with few exceptions<sup>4–7</sup> there are no direct studies of the pressure and temperature dependence of these reactions. The most direct studies have employed laser-induced fluorescence (LIF) spectroscopy to monitor the disappearance of alkoxy radical.<sup>4,6,7</sup> Indeed, LIF spectra have been extremely useful in kinetic studies of a variety of bimolecular reactions of small alkoxy radicals.<sup>2,8</sup> However, until last year,<sup>6</sup> no one had obtained LIF excitation spectra of any alkoxy radical with more than three carbon atoms, and this fact has hindered investigations of the kinetics of the unimolecular reactions which are expected to dominate the atmospheric chemistry of the larger ( $\geq \text{C}_4$ ) alkoxy radicals. It might be supposed that C<sub>4</sub> and larger alkoxy radicals do not fluoresce and that their (ambient temperature) spectra are lacking in structure. However, an old report of fluorescence emission from *tert*-butoxy radical gives lie to these assumptions,<sup>9</sup> and very recently the LIF excitation spectrum of *tert*-butoxy radical was reported and used as a tool for kinetic studies.<sup>6</sup>

In addition to the fascinating variety of the thermal chemistry of alkoxy radicals, small alkoxy radicals are known to exhibit

## SCHEME 1



mode-specific rates of dissociation on the ground<sup>10</sup> and electronic excited state surfaces.<sup>11,12</sup> While it has long been believed that excited state methoxy radical ( $\text{CH}_3\text{O}^*$ ) predissociates upon excitation of more than about six quanta of C–O stretch,<sup>13</sup> recent experiments have revealed that the predissociation rates of  $\text{CH}_3\text{O}^*$  and  $\text{CD}_3\text{O}^*$  have sharp onsets and are extremely mode-dependent.<sup>11,12</sup> This photochemistry has also been the subject of renewed theoretical interest.<sup>14</sup>

In this paper we report observations of LIF excitation spectra of *tert*-butoxy and 2-butoxy. Our observations of *tert*-butoxy confirm and extend the recently published spectrum of Blitz and co-workers.<sup>6</sup> The LIF spectra of 2-butoxy radical represents the first report of the fluorescence of this species. These spectra obtained at 213 K exhibit abundant but highly overlapped vibronic structure from which only a very preliminary analysis can be made. Fluorescence lifetimes are reported for both radicals.

## II. Experimental Section

Alkoxy radicals were generated from the 355 nm photolysis of the appropriate butyl nitrites; this is a general method for

\* To whom correspondence should be addressed. E-mail: tsdibble@mailbox.syr.edu.

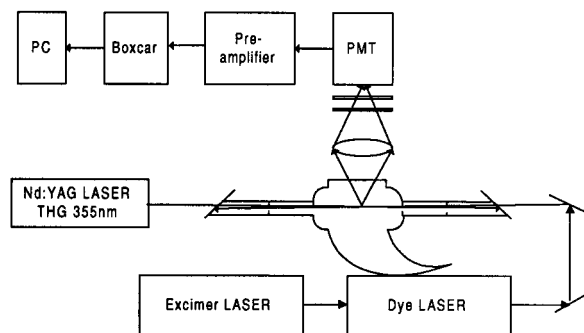


**Figure 1.** Diagram of the experimental setup.

generating alkoxy radicals.<sup>15,16</sup> *tert*-Butyl nitrite and 2-butyl nitrite were prepared by the dropwise addition of concentrated sulfuric acid to a saturated solution of  $\text{NaNO}_2$  and the corresponding butanol.<sup>17</sup> The butyl nitrites appear as pale yellow liquids, which were further purified by three freeze-pump-thaw cycles followed by trap-to-trap distillation. Verification of the identity and purity of the nitrites was done by observing their IR,<sup>18</sup> UV,<sup>15,19</sup> and NMR<sup>18</sup> spectra.

A schematic diagram of the experimental apparatus is shown in Figure 1. The reaction cell consists of a Pyrex tube with an inner diameter of 57 mm surrounded by a cooling jacket of 110 mm diameter. It has two 63 mm long glass sidearms to which quartz windows are attached at Brewster's angle. Two light baffles are located inside each arm. The photolysis and probe laser beams counterpropagate collinearly through the inner Pyrex tube. The temperature of the cell is varied between 288 and 213 K by flowing ethanol through the cooling jacket. The temperature of the cooling liquid is controlled by a temperature bath (Neslab ULT-80). A flow controller (MKS 247) regulates the gas mixture flowing into the cell, and a capacitance manometer (MKS 662) indicates the pressure in the reaction cell. The flow rate of the gas mixture for all the experiments is ca. 30 sccm. Based on the constant pressure in the reaction cell of 5.6 Torr, the photolysis energy of 15 mJ, and the shape of the laser beam, the initial radical concentration is estimated to be  $2 \times 10^{14}$  radicals  $\text{cm}^{-3}$ . The carrier gas is nitrogen (MG 99.999%) used without further purification.

A frequency-tripled Nd:YAG laser (Quanta-Ray DCR-2) provides  $\sim 15$  mJ photolysis energy per pulse at 355 nm. The

output of the photolysis beam is collimated and focused by a lens. The output of the probe dye laser (Lambda Physik FL3002), pumped by excimer laser (Lextra 100, 308 nm XeCl), is about 1–2 mJ per pulse at 4 Hz repetition rate, with tuning range of 335–400 nm obtained by the use of three different dyes: PTP, DMQ, and PPI. The dye laser wavelength was scanned at  $0.04 \text{ nm s}^{-1}$ . We do not have a simultaneous frequency calibration for the dye laser. In experiments where we measured two-photon LIF excitation spectrum of NO near 454 nm<sup>20</sup> the nominal laser frequency was  $10 \text{ cm}^{-1}$  larger than the true frequency. In the butoxy experiments the frequency was always reproducible to  $3 \text{ cm}^{-1}$ . The delay time between the two lasers is controlled by a pulse generator (SRS DG535) and varied between 0.5 and 50  $\mu\text{s}$ . The fluorescence signal is collected perpendicularly to the laser beams by a pair of 2 in. diameter lenses; a  $f = 100$  mm lens collimates the emission and a  $f = 150$  mm lens focuses it on a photomultiplier tube (Hamamatsu R212) connected with an amplifier (EG&G ORTEC 114). Two filters above the lenses and a Wood's horn at the bottom of the cell opposite the photomultiplier tube are used to reduce the scattered laser light. The filters were a long-pass filter (either CVILP-380 or LP-400) and medium band interference filter (either CVIF-70-400.0 or F-70-425.0). The amplifier output is integrated by a boxcar averager (SRS SR270), digitized by A/D converter (SRS SR245), and sent to a PC for further data processing. A 10-point smoothing has been applied to the data before plotting. Fluorescence decay curves are acquired using the scanning mode of the boxcar.

### III. Results and Discussion

**A. LIF Spectra of *tert*-Butoxy and 2-butoxy.** Figure 2 shows vibronically structured LIF excitation spectrum of *tert*-butoxy ( $\bar{B}-\bar{X}$ )<sup>21–23</sup> in the range 330–400 nm. Three different dyes were used to obtain this scanning range. The spectrum shown here was obtained from the experimental spectrum by subtracting a background consisting of the spectrum obtained when *tert*-butyl nitrite was exposed only to the probe (dye) laser. The overlapped spectra from two different dyes show that spectra are repeatable, and that the small peaks represent LIF signal rather than random noise. In Figure 2, 16 vibronic bands in two progressions are labeled. Bands in the region 335–360 nm, which were first observed by Blitz et al.,<sup>6</sup> are noted with an asterisk in Figure 2;

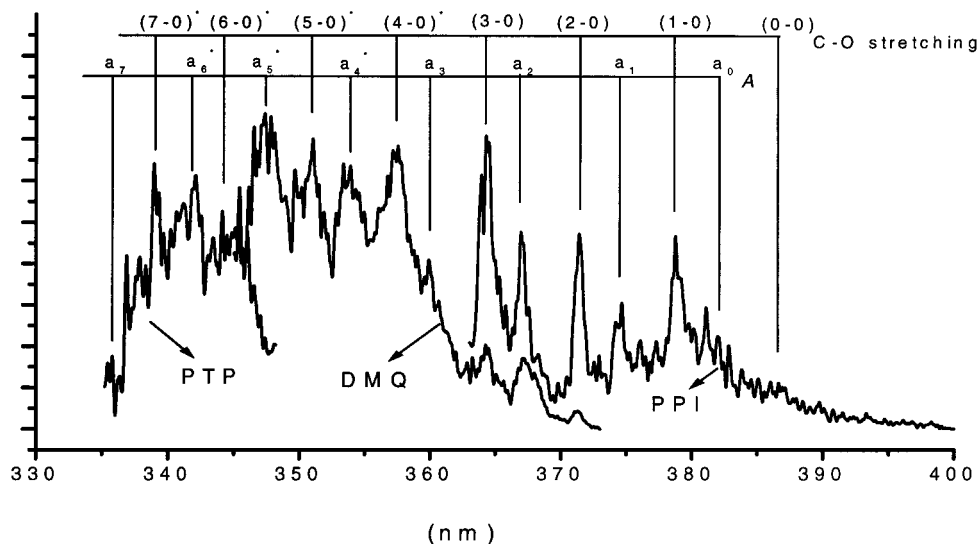


**Figure 2.** LIF excitation spectra of *tert*-butoxy at 213 K. 5% *tert*-butyl nitrite in  $\text{N}_2$  at a total pressure of 5.6 Torr. The delay time between the photolysis laser and the probe laser is 10  $\mu\text{s}$ . Three different dyes (PTP, DMQ, and PPI) were used to cover the desired tuning range. Spectra were corrected for the background. Bands observed in ref 6 denoted by \*.

**TABLE 1: Observed Band Origins of *tert*-Butoxy  $\tilde{B}-\tilde{X}$  ( $\text{cm}^{-1}$ )<sup>a</sup>**

label	band origin	vibrational intervals
C–O stretching ( $\nu'-\nu''$ )		
0–0	25 866	
		536
1–0	26 402	
		524
2–0	26 926	
		524
3–0	27 450	
		522
4–0*	27 972	
		522
5–0*	28 494	
		517
6–0*	29 011	
		505
7–0*	29 516	
progression A		
a <sub>0</sub>	26 178	
		546
a <sub>1</sub>	26 724	
		528
a <sub>2</sub>	27 252	
		526
a <sub>3</sub>	27 778	
		511
a <sub>4</sub> *	28 289	
		505
a <sub>5</sub> *	28 794	
		497
a <sub>6</sub> *	29 291	
		495
a <sub>7</sub>	29 786	

<sup>a</sup> \* denotes the bands observed in ref 6.

our observations are in good agreement with theirs. Bands in the longer wavelength portion of the spectrum are better resolved than those in the shorter wavelength region. By analogy to the spectra of smaller alkoxy radicals<sup>4,22,24–30</sup> ( $\text{CH}_3\text{O}$ ,  $\text{C}_2\text{H}_5\text{O}$ ,  $2\text{-C}_3\text{H}_7\text{O}$ ,  $1\text{-C}_3\text{H}_7\text{O}$ ), the dominant progression in Figure 2 is assigned to the C–O stretching vibration. The average vibrational band interval is  $521\text{ cm}^{-1}$ , the same as that obtained by Blitz and co-workers,<sup>6</sup> and little anharmonicity is observed. We tentatively assign the transition origin, in the following noted as (0–0), at  $25\,866\text{ cm}^{-1}$  ( $386.6\text{ nm}$ ). A weaker progression

(labeled progression A in Figure 2) originates  $\sim 312\text{ cm}^{-1}$  higher than the C–O progression and possesses an average band interval of  $515\text{ cm}^{-1}$ . The spectra of all small alkoxy radicals show an analogous progression<sup>4,8,28,29</sup> ( $\text{CH}_3\text{O}$ ,  $\text{C}_2\text{H}_5\text{O}$ ,  $2\text{-C}_3\text{H}_7\text{O}$ ,  $1\text{-C}_3\text{H}_7\text{O}$ ), but the assignment of this progression has not been clear. In the present work we make no mode assignment to progression A, in which all bands are labeled as  $a_0$ ,  $a_1$ ,  $a_2$ , ... Numerous other bands remain unassigned in Figure 2. The observed band origins are listed in Table 1 along with the vibrational band intervals of each progression. Peak locations should be accurate to within  $5\text{ cm}^{-1}$ ; however, band origins for *tert*-butoxy have a larger uncertainty due to spectral congestion.

Figure 3 shows the overall LIF excitation spectrum of 2-butoxy ( $\tilde{B}-\tilde{X}$ ) between 345 and 390 nm. No fluorescence signal was observed beyond this region. This spectrum is corrected for laser power variations by dividing the experimental spectrum by the background spectrum obtained with the photolysis laser blocked. The region of overlap of the two dyes shows that the spectra are repeatable and that small peaks are more than just noise. The spectrum of 2-butoxy is much less congested than the short-wavelength portion of the *tert*-butoxy spectrum. Fifteen vibronic bands in four progressions are labeled in Figure 3. As with *tert*-butoxy, the strongest progression is assigned to the C–O stretching mode. The average band interval,  $\nu'_{\text{C-O}}$ , is  $567\text{ cm}^{-1}$ . The transition origin is assigned to the peak at  $381.9\text{ nm}$  ( $26\,185\text{ cm}^{-1}$ ). Another strong progression, labeled A, originates  $277\text{ cm}^{-1}$  higher than the C–O progression and possesses an average band interval  $617\text{ cm}^{-1}$ . This progression clearly does not originate from a C–O stretch progression. From Figure 3, we can see that band structures in this progression are different from those in the C–O progression. For instance, the peaks at  $361.0\text{ nm}$  ( $a_2$ ) and  $369.2\text{ nm}$  ( $a_1$ ) are split to form a shoulder  $20\text{ cm}^{-1}$  to the blue of each peak. By contrast, each peak in the C–O progression has a red shoulder, which can be seen clearly in Figure 4. In addition, the band intervals are significantly different from those in the C–O progression. Even the smallest band interval ( $612\text{ cm}^{-1}$ ) in this progression is bigger than the biggest one ( $589\text{ cm}^{-1}$ ) in the C–O progression. Two other weak progressions in Figure 3 are labeled B and C with average band intervals  $590$  and  $552\text{ cm}^{-1}$ , respectively. Observed band origins are listed in Table

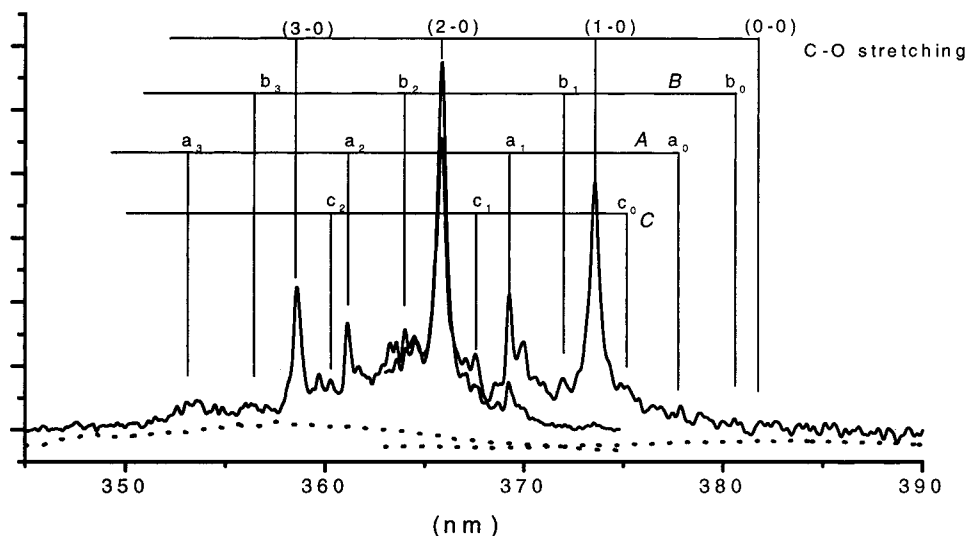


**Figure 3.** LIF excitation spectra of 2-butoxy at 213 K. 5% 2-butyl nitrite in  $\text{N}_2$  at a total pressure of 5.6 Torr. The delay time between the photolysis laser and the probe laser is  $10\ \mu\text{s}$ . Two different dyes (DMQ and PPI) were used to obtain the desired tuning range. Spectra were corrected for the background.

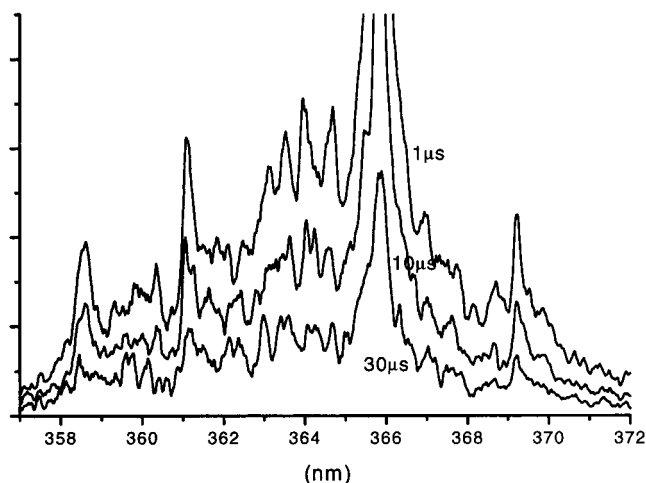


**Figure 4.** Time-resolved LIF spectra of 2-butoxy in the range 357–372 nm. Spectra from top to bottom were measured at delay times of 1, 10, and 30  $\mu$ s, respectively. 5% 2-butyl nitrite in  $N_2$  at a total pressure of 5.6 Torr.

**TABLE 2: Observed Band Origins of 2-butoxy  $\tilde{B}-\tilde{X}$  ( $cm^{-1}$ )**

label	band origin	vibrational intervals
C–O stretching ( $v'-v''$ )		
0–0	26 185	
1–0	26 774	589
2–0	27 337	549
3–0	27 886	
progression A		
$a_0$	26 462	624
$a_1$	27 086	615
$a_2$	27 701	612
$a_3$	28 313	
progression B		
$b_0$	26 278	607
$b_1$	26 885	588
$b_2$	27 473	576
$b_3$	28 049	
progression C		
$c_0$	26 650	556
$c_1$	27 206	549
$c_2$	27 755	

2. Vibrational intervals show that there is a clear anharmonic tendency in each progression, which was not observed for *tert*-butoxy.

It is clear that our assignments of the transition origins for *tert*-butoxy and 2-butoxy are not conclusive. Examining the spectra shown in Figures 2 and 3, one might think to assign the transition origin of *tert*-butoxy to the band labeled (1–0) instead of the band (0–0) (25 866  $cm^{-1}$ , as suggested in this paper). Similarly, the transition origin of 2-butoxy in Figure 3 is either at band (0–0) (26 185  $cm^{-1}$ , which is preferred in this paper) or at band (1–0). There are three reasons that influence our assignments. First, all the labeled progressions (not just the C–O stretches) appear to originate to the red of the (1–0) peaks. Second, the shapes of the (1–0) and (0–0) peaks for *tert*-butoxy, at least, are similar. Third, although it might seem unreasonable that such weak bands be labeled the origin, the origin band of 2-propoxy radical is also weak.<sup>4,8</sup>

**TABLE 3: Transition Origin and C–O Stretching Frequency ( $cm^{-1}$ ) of Alkoxy Radicals<sup>a</sup>**

radical	transition origin	the excited-state C–O str freq	ref
$CH_3O$	31 540	678	25
	31 540	683	32
	31 530	680	29
	31 614.5	660	26, 30
$C_2H_5O$	29 204	596	28
	29 200	600	29
$n-C_3H_7O$	29 000	450 $\pm$ 50	9
	28 637	580 $\pm$ 10	8
$i-C_3H_7O$	27 140		31
	27 168	560 $\pm$ 10	8
	27 167	560	32
		560 $\pm$ 10	4
$2-C_4H_9O$	26 185	567 $\pm$ 10	this work
$t-C_4H_9O$	25 866	521 $\pm$ 10	this work
		500 $\pm$ 20	6

<sup>a</sup> The excited states of  $C_2$ – $C_4$  radicals have been variously labeled either  $\tilde{A}-\tilde{X}$  or  $\tilde{B}-\tilde{X}$ , but all the data refer to the first bound excited state in the near-UV.

Locations of the known transition origins of the  $C_1$ – $C_4$  alkoxy radicals are listed in Table 3. It can be seen that with the increasing of number of carbon atoms in alkoxy radicals, the transition origin shifts to lower energy. The same effect is observed upon going from a primary to a secondary propoxy radical, and from a secondary to a tertiary butoxy radical. The C–O stretching frequency in the electronic excited state decreases as the number of carbons increases, presumably reflecting the increasing reduced mass effect on the oscillator.

#### B. Time Evolution of Spectra and Temperature Effects.

Delay times in the range 500 ns to 30  $\mu$ s between the photolysis laser and probe laser have been used to obtain time-resolved spectra of *tert*-butoxy and 2-butoxy. Figure 4 shows a typical time-resolved LIF spectrum. From the changes in the spectra, it is clear that the radicals have not been thermalized after 10  $\mu$ s.

All spectra shown in this paper were obtained in 213 K. Room temperature spectra were also measured. For *tert*-butoxy, room temperature spectra are much more overlapped than that at 213 K, and only the strongest bands at 341.4, 357.5, 364.3, 378.7 nm can be clearly distinguished. However, there is no such obvious difference in 2-butoxy spectra.

**C. Fluorescence Lifetimes.** Fluorescence lifetimes were measured for numerous strong bands of each radical. From the quality of the fits of the measured fluorescence curves it can be concluded that fluorescence decay follows single-exponential behavior. The standard error on the fits is typically less than  $\pm 3$  ns. For these studies, the total pressure of the gas mixture (2% alkyl nitrite in  $N_2$  at 213 K) in the chamber was varied from 10 to 1.7 Torr. Zero-pressure fluorescence lifetimes of each vibrational level was obtained by extrapolating least-squares fits of the measured data. These extrapolations had a maximum statistical error of 7%; we assume a minimum error of  $\pm 10$  ns. Figure 5 shows the pressure dependence of fluorescence lifetimes of three different vibrational levels of 2-butoxy. Table 4 lists the complete set of zero-pressure lifetimes for both radicals. It can be seen that fluorescence lifetimes of *tert*-butoxy (131–172 ns) are longer than those of 2-butoxy (70–99 ns), but much shorter than those of other alkoxy radicals, whose lifetimes range from 2.6  $\mu$ s for methoxy<sup>12,13,23</sup> to 300–500 ns for 2-propoxy radicals.<sup>8,33</sup> Blitz et al.<sup>6</sup> reported a fluorescence lifetime for *tert*-butoxy of ca. 500 ns. We have no explanation for the large difference between our result and theirs.

While fluorescence lifetimes are somewhat mode-dependent, this is not likely due to the onset of predissociation, which has



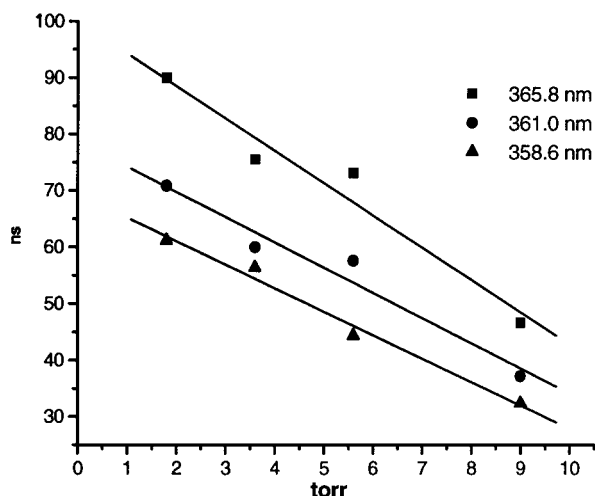


**Figure 5.** Pressure dependence fluorescence lifetimes of 2-butoxy at three different excitation wavelengths. Delay time: 10  $\mu$ s. 5% 2-butyl nitrite in  $N_2$  at a total pressure of 5.6 Torr. As mentioned in the text, error bars on each data point were less than or equal to 3 ns.

**TABLE 4: Zero-Pressure Fluorescence Lifetimes (ns) of Different Vibrational Levels of B State**

radical	label	band origin (nm)	$\tau_0$ ( $\pm$ ions)
<i>tert</i> -butoxy	(4-0)	357.5	172
	(3-0)	364.3	135
	(2-0)	371.4	138
	a <sub>5</sub>	347.3	124
	a <sub>4</sub>	353.4	167
2-butoxy	a <sub>2</sub>	367.0	131
	(3-0)	358.6	70
	(2-0)	365.8	99
	a <sub>2</sub>	361.0	79

(for  $CH_3O$ , at least) a rather more dramatic effect on fluorescence lifetimes. The fluorescence lifetime of jet-cooled  $CH_3O$  exhibits some mode dependence while decreasing by as much as 40% upon excitation of  $\sim 3000\text{ cm}^{-1}$  of vibration in the  $\tilde{A}$  state (well before the onset of predissociation).<sup>12,13,34</sup> The extent of the LIF excitation spectrum of 2-butoxy (4 C–O stretch bands) is narrower than that of ethoxy and 2-propoxy (5 C–O stretch bands),<sup>4,8,28</sup> which is in turn narrower than that of methoxy (6 or 7 C–O stretch bands). Predissociation of excited methoxy radical begins at  $\nu'_{C-O} = 6$  and predissociation essentially eliminates fluorescence from  $\nu'_{C-O} = 8$ .<sup>11,12,34</sup>

#### IV. Conclusions

Laser-induced fluorescence excitation spectra of *tert*-butoxy and 2-butoxy ( $\tilde{B}-\tilde{X}$ ) are observed following laser photolysis of the corresponding butyl nitrites at 355 nm. For *tert*-butoxy, the spectral range studied was extended down to the apparent origin at  $25\,866\text{ cm}^{-1}$  (386.6 nm), far to the red of the region examined in the initial study by Blitz and co-workers (330–360 nm).<sup>6</sup> This enables us to identify two progressions consisting of 16 vibronic bands. Our results for 2-butoxy represent the first observations of electronic spectra for this species. The transition origin of 2-butoxy is tentatively assigned at  $26\,185\text{ cm}^{-1}$  (381.9 nm), and 15 vibronic bands in four progressions are labeled. In each radical the dominant progression is assigned to a C–O stretching vibration, with frequencies for *tert*-butoxy and 2-butoxy radicals of  $\nu'_{C-O} = 521 \pm 10\text{ cm}^{-1}$  and  $\nu'_{C-O} = 567 \pm 10\text{ cm}^{-1}$ , respectively. The other progressions labeled here in the spectrum of 2-butoxy do not originate from C–O stretching mode excitation. Overall fluorescence lifetimes for *tert*-butoxy and 2-butoxy are ca. 150 and ca. 85 ns, respectively.

Mode assignments cannot be made for most of the progressions noted here, and numerous additional bands are evident in the spectra for which progressions cannot be reliably described. Further progress is likely to require analysis of jet-cooled spectra, and the complete analysis of these radicals poses a significant challenge to spectroscopy. It is hoped that this work will aid future investigations of the chemistry and kinetics of alkoxy radicals as well as increasing interest in the spectroscopy and photodissociation dynamics of alkoxy radicals containing more than one or two carbon atoms.

**Acknowledgment.** Our interest in this topic originated in conversations with R. Atkinson; we are in debt to him for his encouragement and for many helpful discussions. This work was funded by the National Science Foundation and by the donors of the Petroleum Research Fund, administered by the American Chemical Society. We are indebted to J. O. Clevenger for designating us as the recipient of the R. W. Field group's surplus Nd:YAG laser. We further thank K. J. Guerin for repeatedly going beyond the call of duty, Dr. J. Chaiken for his advice and encouragement, and D. R. Katz for assistance with some experiments.

#### References and Notes

- Jenkin, M. E.; Hayman, G. D. *Atmos. Environ.* **1999**, *33*, 1275.
- Atkinson, R. *J. Phys. Chem. Ref. Data* 1994, Monograph No. 2.
- Atkinson, R. *Int. J. Chem. Kinet.* **1997**, *29*, 99.
- Balla, R. J.; Nelson, H. H.; McDonald, J. R. *Chem. Phys.* **1985**, *99*, 323.
- Hein, H.; Hoffmann, A.; Zellner, R. *Ber. Bunsen-Ges. Phys. Chem.* **1998**, *102*, 1840.
- Blitz, M.; Pilling, M. J.; Robertson, S. H.; Seakins, P. W. *Phys. Chem. Chem. Phys.* **1999**, *1*, 73.
- Devolder, P.; Fittschen, Ch.; Frenzel, A.; Hippler, H.; Poskrebyshev, G.; Striebel, F.; Viskolcz, B. *Phys. Chem. Chem. Phys.* **1999**, *1*, 675.
- Mund, C.; Fockenberg, C.; Zellner, R. *Ber. Bunsen-Ges. Phys. Chem.* **1998**, *102*, 709.
- Bai, J.; Okabe, H.; Emadi-Babaki, M. K. *J. Photochem. Photobiol. A* **1989**, *50*, 163.
- Geers, A.; Kappert, J.; Temps, F.; Wiebrecht, J. W. *J. Chem. Phys.* **1993**, *99*, 2271.
- Osborn, D. L.; Leahy, D. J.; Neumark, D. M. *J. Phys. Chem. A* **1997**, *101*, 6583.
- Powers, D. E.; Pushkarsky, M.; Miller, T. A. *J. Chem. Phys.* **1997**, *106*, 6878.
- Lin, S.-R.; Lee, Y.-P.; Nee, J. B. *J. Chem. Phys.* **1988**, *88*, 171.
- Cui, Q.; Morokuma, K. *Chem. Phys. Lett.* **1996**, *263*, 54.
- Calvert, J. G.; Pitts, J. N. Jr. *Photochemistry*; Wiley: New York, 1966.
- Reisler, H.; Noble, M.; Wittig, C. In *Molecular Photodissociation Dynamics*; Ashfold, M. N. R., Baggott, J. E., Eds.; Royal Society of Chemistry: London, 1987.
- Organic Syntheses*; Blatt, A. H., Ed.; Wiley: New York, 1943; p 108.
- Sadtler Index*; Bio-Rad Laboratories, Inc., 1973.
- Lahmani, F.; Lardeux, C.; Solgadi, D. *Chem. Phys. Lett.* **1983**, *102*, 523.
- Bray, R. G.; Hochstrasser, R. M.; Wessel, J. E. *Chem. Phys. Lett.* **1974**, *27*, 167.
- There is confusion in the literature over whether the fluorescent near-ultraviolet excited states of alkoxy radicals larger than methoxy are properly labeled  $\tilde{A}-\tilde{X}$ , as is common, or  $\tilde{B}-\tilde{X}$ .<sup>22,23</sup> We shall refer to the transitions of both *tert*-butoxy and 2-butoxy as  $\tilde{B}-\tilde{X}$ .
- Tan, X. Q.; Williamson, J. M.; Foster, S. C.; Miller, T. A. *J. Phys. Chem.* **1993**, *97*, 9311.
- Zhu, X.; Kamal, M. M.; Misra, P. *Pure Appl. Opt.* **1996**, *5*, 1021.
- Wendt, H. R.; Hunziker, H. E. *J. Chem. Phys.* **1979**, *71*, 5202.
- Inoue, G.; Akimoto, H.; Okuda, M. *J. Chem. Phys.* **1980**, *72*, 1769.
- Liu, X. M.; Damo, C. P.; Lin, T.-Y. D.; Foster, S. C.; Misra, P.; Yu, L.; Miller, T. A. *J. Phys. Chem.* **1989**, *93*, 2266.
- Misra, P.; Zhu, X.; Hsueh, C.-Y.; Halpern, J. B. *Chem. Phys.* **1993**, *178*, 377.
- Inoue, G.; Okuda, M.; Akimoto, H. *J. Chem. Phys.* **1981**, *75*, 2060.

- (29) Ebata, T.; Yanagishita, H.; Obi, K.; Tanaka, I. *Chem. Phys.* **1982**, 69, 27.
- (30) Foster, S. C.; Misra, P.; Lin, T.-Y. D.; Damo, C. P.; Carter, C. C.; Miller, T. A. *J. Phys. Chem.* **1988**, 92, 5914.
- (31) Bai, J.; Okabe, H.; Halpern, J. B. *Chem. Phys. Lett.* **1988**, 149, 37.

- (32) Foster, S. C.; Hsu, Y. C.; Damo, C. P.; Liu, X.; Kung, C. Y.; Miller, T. A. *J. Phys. Chem.* **1986**, 90, 6766.
- (33) Ohbayashi, K.; Akimoto, H.; Tanaka, I. *J. Phys. Chem.* **1977**, 81, 798.
- (34) Fuke, K.; Ozawa, K.; Kaya, K.; *Chem. Phys. Lett.* **1986**, 126, 119.